JACS
JOURNAL OF THE AMERICAN CHEMICAL SOCIETY

Subscriber access provided by ISTANBUL TEKNIK UNIV

Article

Comprehensive Investigation of Self-Assembled Monolayer Formation on Ferromagnetic Thin Film Surfaces

Paul G. Hoertz, Jeremy R. Niskala, Peng Dai, Hayden T. Black, and Wei You

J. Am. Chem. Soc., **2008**, 130 (30), 9763-9772 • DOI: 10.1021/ja800278a • Publication Date (Web): 03 July 2008

Downloaded from http://pubs.acs.org on February 8, 2009

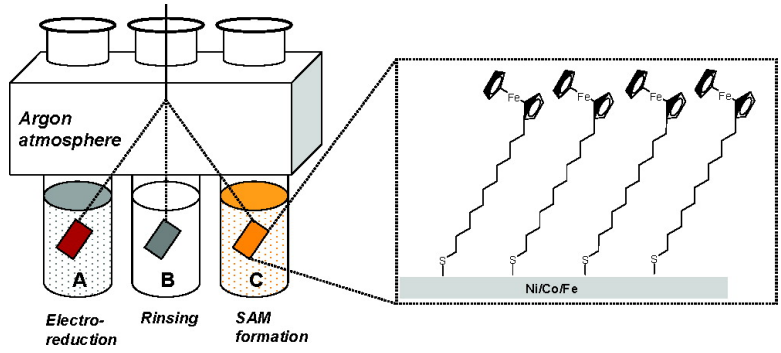

More About This Article

Additional resources and features associated with this article are available within the HTML version:

- Supporting Information
- Access to high resolution figures
- Links to articles and content related to this article
- Copyright permission to reproduce figures and/or text from this article

View the Full Text HTML

ACS Publications
High quality. High impact.

Journal of the American Chemical Society is published by the American Chemical Society. 1155 Sixteenth Street N.W., Washington, DC 20036

J|A|C|S
ARTICLES

Published on Web 07/03/2008

Comprehensive Investigation of Self-Assembled Monolayer Formation on Ferromagnetic Thin Film Surfaces

Paul G. Hoertz, Jeremy R. Niskala, Peng Dai, Hayden T. Black, and Wei You*

Department of Chemistry, University of North Carolina at Chapel Hill, Chapel Hill, North Carolina 27599-3290

Received January 12, 2008; E-mail: wyou@email.unc.edu

Abstract: We report a simple, universal method for forming high surface coverage SAMs on ferromagnetic thin (≤100 nm) films of Ni, Co, and Fe. Unlike previous reports, our technique is broadly applicable to different types of SAMs and surface types. Our data constitutes the first comprehensive examination of SAM formation on three different ferromagnetic surface types using two different surface-binding chemistries (thiol and isocyanide) under three different preparation conditions: (1) SAM formation on electroreduced films using a newly developed electroreduction approach, (2) SAM formation on freshly evaporated surfaces in the glovebox, and (3) SAM formation on films exposed to atmospheric conditions beforehand. The extent of SAM formation for all three conditions was probed by cyclic voltammetry for surfaces functionalized with either (11-thiolundecyl)ferrocene (Fc-$(CH_2)_{11}$-SH) or (11-isocyanoundecyl)ferrocene (Fc-$(CH_2)_{11}$-NC). SAM formation was also probed for straight-chain molecules, hexadecanethiol and hexadecaneisocyanide, with contact angle measurements, X-ray photoelectron spectroscopy, and reflection−absorption infrared spectroscopy (RAIRS). The results show that high surface coverage SAMs with low surface-oxide content can be achieved for thin, evaporated Ni and Co films using our electroreduction process with thiols. The extent of SAM formation on electroreduced films is comparable to what has been observed for SAMs/Au and to what we observe for SAMs/Ni, Co, and Fe samples prepared in the glovebox.

Introduction

Self-assembled monolayers (SAMs) have been widely studied and well-characterized on gold and other inert metal surfaces such as Pt, Ag, and Pd.[1,2] Surface attachment is typically carried out by using alkyl or aryl thiols but has also been achieved via isocyanides, selenols, and so on.[1−4] Self-assembled monolayers are also known to form readily on various metal/native oxide surfaces, such as Al_2O_3, TiO_2, ZrO_2, SiO_2, and Fe_2O_3, typically using carboxylate, phosphonate, hydroxamate, or silane surface attachment chemistries.[5−9] Self-assembly of alkyl/aryl thiols on pristine, oxide-free transition metal surfaces, such as Ni, Co, and Fe, however, has been met with limited success mainly due to the presence of the native oxide which inhibits the formation of direct sulfur−metal linkages.[10] As a result, the majority of literature reports involving SAMs on Ni, Co, and Fe have utilized carboxylates, phosphonates, or silanes for binding to the native oxide surface, while those that involve bare surfaces typically rely on gas-phase adsorption of surfactants.[7,8,11−13] In a few reports, the native oxide of Ni and Fe has been attempted to be removed by electrochemical reduction of the oxide layer under acidic or basic aqueous conditions.[10,14−17] Surprisingly, the electrochemical reduction of the surface and transfer of the substrate to the SAM molecule solution has typically been carried out under atmospheric conditions in spite of the fact that reformation of the native oxide is known to be rapid.[10,11,14] In two of these reports, the electroreduction was performed under either acidic[16,17] or basic[15] aqueous conditions, while SAM formation was carried out either in situ[15] or by pulling the substrate through a top layer of neat thiol.[16,17] In both instances, the broad applicability of the technique is significantly limited by the requirement that the SAM molecules be either slightly miscible[15] or completely immiscible[16,17] with the aqueous layer.

(1) Smith, R. K.; Lewis, P. A.; Weiss, P. S. *Prog. Surf. Sci.* **2004**, *75*, 1.
(2) Love, J. C.; Estroff, L. A.; Kriebel, J. K.; Nuzzo, R. G.; Whitesides, G. M. *Chem. Rev.* **2005**, *105*, 1103.
(3) Henderson, J. I.; Feng, S.; Bein, T.; Kubiak, C. P. *Langmuir* **2000**, *16*, 6183.
(4) Monnell, J. D.; Stapleton, J. J.; Jackiw, J. J.; Dunbar, T.; Reinerth, W. A.; Dirk, S. M.; Tour, J. M.; Allara, D. L.; Weiss, P. S. *J. Phys. Chem. B* **2004**, *108*, 9834.
(5) Hoertz, P. G.; Mallouk, T. E. *Inorg. Chem.* **2005**, *44*, 6828.
(6) Onclin, S.; Ravoo, B. J.; Reinhoudt, D. N. *Angew. Chem., Int. Ed.* **2005**, *44*, 6282.
(7) Yee, C.; Kataby, G.; Ulman, A.; Prozorov, T.; White, H.; King, A.; Rafailovich, M.; Sokolov, J.; Gedanken, A. *Langmuir* **1999**, *15*, 7111.
(8) Helmy, R.; Wenslow, R. W.; Fadeev, A. Y. *J. Am. Chem. Soc.* **2004**, *126*, 7595.
(9) Folkers, J. P.; Gorman, C. B.; Laibinis, P. E.; Buchholz, S.; Whitesides, G. M.; Nuzzo, R. G. *Langmuir* **1995**, *11*, 813.
(10) Mekhalif, Z.; Riga, J.; Pireaux, J.-J.; Delhalle, J. *Langmuir* **1997**, *13*, 2285.
(11) Lee, Y.; Morales, G. M.; Yu, L. *Angew. Chem., Int. Ed.* **2005**, *44*, 4228.
(12) Fadeev, A. Y.; McCarthy, T. J. *J. Am. Chem. Soc.* **1999**, *121*, 12184.
(13) Kataby, G.; Prozorov, T.; Koltypin, Y.; Cohen, H.; Sukenik, C. N.; Ulman, A.; Gedanken, A. *Langmuir* **1997**, *13*, 6151.
(14) Mekhalif, Z.; Laffineur, F.; Couturier, N.; Delhalle, J. *Langmuir* **2003**, *19*, 637.
(15) Bengio, S.; Fonticelli, M.; Benitez, G.; Creus, A. H.; Carro, P.; Ascolani, H.; Zampieri, G.; Blum, B.; Salvarezza, R. C. *J. Phys. Chem. B* **2005**, *109*, 23450.
(16) Stratmann, M. *Adv. Mater.* **1990**, *2*, 191.
(17) Volmer, M.; Stratmann, M.; Viefhaus, H. *Surf. Interface Anal.* **1990**, *16*, 278.

 © 2008 American Chemical Society

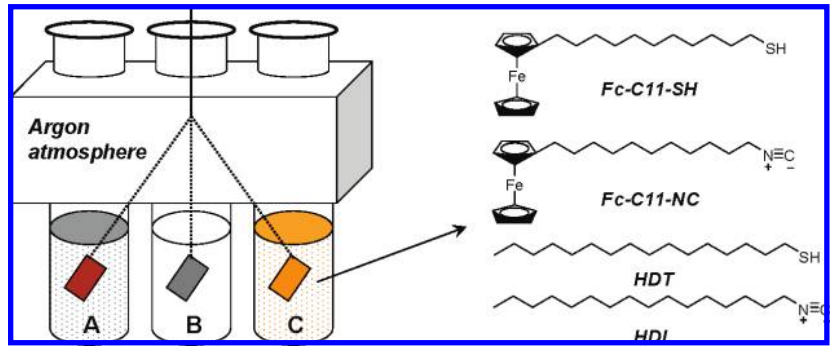

Figure 1. Left: three-chamber design. **A**, electroreduction; **B**, rinsing; **C**, SAM formation. Right: structures of molecules studied.

Herein, we report a simple, universal method for forming high surface coverage SAMs on ferromagnetic thin (≤100 nm) films of Ni, Co, and Fe. Unlike previous reports, our technique is broadly applicable to several different SAMs and surface types. Our data constitutes the first comprehensive examination of SAM formation on three different ferromagnetic surface types using two different surface-binding chemistries (thiol and isocyanide) and three different preparation conditions: glovebox, electroreduction, and atmosphere. Previous reports have suggested that isocyanides and thiols bind well to Ni surfaces.[10,11,14,18,19] Literature reports for SAMs on Co and Fe are extremely limited but suggest that thiolated SAMs can bind to these surfaces.[16,17,20] For glovebox samples, the thin films are removed from the evaporator under an inert atmosphere and submerged in SAM molecule solutions to avoid native oxide formation. For atmosphere samples, the thin films are removed from the glovebox and SAM formation is carried out after native oxide formation. For electroreduction samples, the native oxide is removed electrochemically under an argon atmosphere and the thin film is then transferred to the SAM molecule solution all under an inert atmosphere. A key advancement is the ability to utilize electroreduction techniques on thin films as opposed to bulk metal samples. Thin films are a highly desirable platform for incorporating self-assembled monolayer junctions into large-scale molecular electronic devices. In this paper, we focus on ways to control and minimize the oxide content at the SAM−metal interface because the electronic structure of this interface will inevitably influence the tunneling behavior of the molecular junction in molecular electronic devices.[20]

Experimental Section

Preparation of SAMs on Ferromagnetic Surfaces. Nickel, iron, and cobalt metal films (50 or 100 nm) were prepared by thermal evaporation ($P_{initial} = 2-4 \times 10^{-6}$ mbar; $P_{deposition} = 2-8 \times 10^{-6}$ mbar) on top of a 25 nm titanium adhesion layer (2 Å/s) on a SiO_x/Si wafer (Si <100>, 1 μm thick oxide on one side, Addison Engineering). Ni, Fe, and Co were deposited at 1−1.5 Å/s. The evaporation boats were purchased from RD Mathis; the specific boat for Ni, Co, and Fe evaporation was an alumina-coated tungsten boat (type S1AO-W to avoid alloying of the metals with tungsten), while that for Ti and Au were tungsten boats (type S4-015 W and S42-015W, respectively). Gold (99.999%), nickel (99.98%), cobalt (99.95%), and iron (99.95%) pellets (1/8" × 1/8") were purchased from Kurt J. Lesker, Inc. Titanium slugs (99.995%, 3.175 mm × 3.175 mm) were purchased from Alfa Aesar. Thermal evaporations were performed with an MBraun evaporator contained within an MBraun nitrogen glovebox such that freshly evaporated thin films could be removed from the evaporator chamber under a nitrogen atmosphere. Thicknesses of films were determined using a quartz crystal microbalance located just below the substrate holder in the evaporator. Tooling factors were determined by measuring the true thicknesses of films with a profilometer; the films were deposited through a TEM grid (Ted Pella, Item No. 1GC50, 50 square mesh) shadow mask that was secured to the surface with Kapton tape. X-ray diffraction spectra were obtained for the M/Ti/SiO_x/Si thin films (100 nm for Ni, Co, and Fe; 50 nm for Au; 25 nm Ti for all cases) using a Rigaku multiplex powder diffractometer with Ni-filtered Cu Kα radiation (1.5418 Å) over the range $2\theta = 10-85°$. The evaporated metal films were observed to grow with either a ⟨111⟩ texture (Au, Ni, and Co) or ⟨110⟩ texture (Fe).[21] The grain sizes for the thin films were deduced from the X-ray diffraction data using the Scherer equation: Ni (7.0 Å), Co (5.1 Å), Fe (8.6 Å), and Au (9.3 Å).

For SAMs prepared in the glovebox, a 1 or 10 mM SAM solution in ethanol (100%, Pharmco) was placed in a vial with septum-containing screw cap (VWR part 15900-008), purged with Argon for 1 h, and then brought into the glovebox (O_2 levels ≤2 ppm). The freshly evaporated M/Ti/SiO_x/Si film was immediately submerged in the SAM solution and allowed to react inside of the glovebox (time was typically for 24−48 h). For SAMs prepared under atmospheric conditions, the M/Ti/SiO_x/Si film was removed from the glovebox and exposed to atmospheric conditions for at least 30 min prior to submersion in the SAM solution and stored under atmospheric conditions.

For SAMs prepared via electroreduction, the M/Ti/SiO_x/Si film was removed from the glovebox and secured to a glass microscope slide (typically substrate size = 1.5 × 2.5 cm) using UV-epoxy (Epotek OG116-31). UV irradiation was carried out by exposing both sides of the sample for ∼10 min; through-glass irradiation was performed by placing the substrate on a small, clean plastic Petri dish at an angle of ∼15°. The purpose of the UV-epoxy is to ensure that the applied potential during the electroreduction step is provided to the exposed metal surface and not to the sides and bottom of the silicon substrate; lower SAM surface coverages were observed when the M/Ti/SiO_x/Si sample was not secured to glass with UV-epoxy especially in the cases of Co and Fe. A custom-built (Quark Glass, Inc.), three-chambered piece of glassware was used to perform the electroreduction procedure under an argon atmosphere (Figure 1). The SAM solution (20 mL) was prepared and placed in the right-most chamber, deionized water (30 mL) was placed in the central chamber, and aqueous electrolyte was placed in the left-most chamber (20 mL). 24/40 rubber septa were used to seal the openings of the three chambers. For the left-most chamber, a wire soldered to a Ni-plated alligator clip was inserted through the rubber septum to make an electrical connection to the reference electrode. A Ni-plated alligator clip was soldered to a PTFE-

(18) Vogt, A. D.; Han, T.; Beebe, T. P. *Langmuir* **1997**, *13*, 3397.
(19) Friend, C. M.; Stein, J.; Muetterties, E. L. *J. Am. Chem. Soc.* **1981**, *103*, 767.
(20) Caruso, A. N.; Wang, L. G.; Jaswal, S. S.; Tsymbal, E. Y.; Dowben, P. A. *J. Mater. Sci.* **2006**, *41*, 6198.
(21) Ghebouli, B.; Cherif, S.-M.; Layadi, A.; Helifa, B.; Boudissa, M. *J. Magn. Magn. Mater.* **2007**, *312*, 194.

coated stainless steel rod (1/16 in. diameter, McMaster-Carr) for an electrical connection to the platinum gauze counter electrode. A bent (~30°), PTFE-coated stainless steel rod (1/16 in. diameter) with soldered, Ni-plated alligator clip was inserted through the rubber septum located at the central chamber opening to make an electrical connection to the working M/Ti/SiO_x/Si/epoxy/glass electrode. The chambers were purged with argon for 2 h prior to the electroreduction step by using three 10" stainless steel needles that penetrate through the rubber septa and are submerged in the solution within each chamber; a short needle was placed in one of the septa to avoid pressure build-up. During electroreduction, purging was continued only at the SAM solution chamber. During the entire purging process, the M/Ti/SiO_x/Si/epoxy/glass electrode was submerged in the central chamber's deionized water to discourage exposure to semivolatile SAMs like hexadecanethiol. This process was used to avoid gas-phase hexadecanethiol from depositing on the metal surface prior to electroreduction. Following electroreduction and working electrode transfer into the SAM solution, purging was continued for the entire duration of the SAM formation.

The applied potential during the electroreduction was provided by a Bioanalytical Systems (BAS) Epsilon potentiostat, and currents were measured as a function of time in the controlled electrolysis mode. The applied potential was increased until the initial current reached 2−3 mA. For Ni and Fe, the electrolyte was 0.1 M NaOH. For Co, the electrolyte was chosen to be 0.1 M KH_2PO_4 (pH = 8, adjusted with NaOH (aq)) and the applied potential was typically −0.95 − (−1.0 V) versus Ag/AgCl. Significant etching of the Co film was evident when 0.1 M NaOH (aq) was used as the electrolyte; etching was not apparent by eye with 0.1 M KH_2PO_4 (pH = 8). The electroreduction time was typically 10 min. After electroreduction, the working electrode was transferred to the middle chamber for rinsing of the electrode using the rigid, PTFE-coated stainless steel rod and then transferred to the SAM solution for SAM formation. At the completion of SAM formation, the working electrode was rinsed. All samples (i.e., glovebox, electroreduction, and atmospheric samples) were rinsed well with ethanol followed by acetone, sonicated for 30 s in THF, then rinsed again with acetone and ethanol, and then dried in a nitrogen stream. After characterization by CV and/or contact angle measurements, SAM samples were stored in a nitrogen atmosphere glovebox (1−2 ppm O_2) in a parafilm-encapsulated plastic Petri dish.

Characterization of SAMs on Ferromagnetic Surfaces. Surface coverage measurements were made by performing cyclic voltammetry in a three-electrode cell with Fc-$(CH_2)_{11}$-SH or Fc-$(CH_2)_{11}$-NC derivatized M/Ti/SiO_x/Si as the working electrode. The electroactive area of the working electrode was defined by a viton O-ring (7 mm outer diameter) placed in a 7 mm hole of a 1 mm thick Delrin spacer. A 1" inner diameter viton O-ring was then placed about the Delrin hole followed by a glass joint (Chemglass, part CG-124-05). The entire arrangement was held together by a clamp (Chemglass, part CG 150-06). The electrolyte solution (0.1 M tetrabutylammonium hexafluorophosphate in dry, distilled tetrahydrofuran) was then placed inside the glass joint along with a platinum gauze counterelectrode and a BAS nonaqueous reference electrode (Ag wire in 0.01 M $AgNO_3$/0.1 M tetrabutylammonium hexafluorophosphate in acetonitrile). External electrical contact to the working electrode was made via an alligator clip. The dryness of the THF electrolyte was critical for attaining good CV data with Co films and was less critical for Ni and Fe. As a result, all components of the apparatus were dried with a heat gun prior to CV experiments performed on Co films. Cyclic voltammograms were attained by scanning the potential from −0.2 to 0.4 V and back at a particular scan rate (typically 0.2 or 0.5 V/s). Integration of the area under the redox waves was performed after subtracting away the baseline current that results from nonfaradaic processes.

Contact angle measurements were performed using a CAM 200 optical contact angle meter (KSV Instruments, Ltd.). A 5 μL drop of deionized water was placed atop the SAM/surface. The contact angle data reported are averages of 4−8 contact angles; standard deviations fall within the range ±0.5−2.0.

X-ray photoelectron spectroscopy (XPS) measurements were carried out at the Chapel Hill Analytical and Nanofabrication Laboratory (CHANL) at UNC using a Kratos Analytical Axis Ultra spectrometer with monochromatized X-ray Al Kα radiation (1486.6 eV). Survey scans were performed with a step size of 1 eV and a pass energy of 80 eV, while region scans were performed with a step size of 0.1 eV and a pass energy of 20 eV. The peaks of region scans were fit with a Gaussian−Lorentzian product function that was weighted 30% Lorentzian. The binding energies of the O 1s, C 1s, and S 2p XPS peaks were referenced to metal $2p_{3/2}$ photoelectron peaks at 852.7 (Ni), 778.3 (Co), and 707 eV (Fe) for oxide-free metal surfaces.[22] Surfaces functionalized with hexadecanethiol (10 mM SAM molecule solution concentration) were prepared under glovebox, electroreduction, and atmosphere conditions. The stability of the SAM and the surface beneath the SAM was studied as a function of exposure time to the ambient. The first data point was attained by removing the samples from their storage conditions and transporting the samples to the XPS location (total loading time ~30 min−1 h). Electroreduction and glovebox samples were stored under a nitrogen atmosphere in a glovebox. Atmospheric samples were removed from their SAM molecule solutions and rinsed with solvent an hour prior to XPS analysis.

AFM images were collected using a Multimode IIIa Atomic Force Microscope (Veeco Metrology Group). The microscope was operated in tapping mode at ambient conditions (T = 21 °C, RH = 45%), using silicon cantilevers (Mikromasch, Part No. NSC14/no Al) with resonance frequencies of approximately 160 kHz and tip radii less than 10 nm. To ensure accuracy, multiple images were taken of the same sample but in different areas.

Reflection−absorption infrared spectroscopy (RAIRS) was conducted at the Nanochemistry Laser and Vibrational Spectroscopy Laboratory located at North Carolina State University in the Department of Chemistry. Spectra were recorded using a Bio-Rad-Digilab FTS-3000 Fourier transform infrared (FT-IR) spectrometer using a Varian Universal variable grazing angle reflectance attachment with a ZnSe polarizer having a normal spectral window of 650−7500 cm^{-1}. The infrared light was focused onto the photodiode of a liquid nitrogen-cooled, narrow band mercury−cadmium−telluride (MCT) detector with a normal spectral response of 650−7000 cm^{-1}. The angle of incidence used was 70° with respect to the surface normal. An infrared polarizer was used to obtain *p*-polarized light. The spectrometer and attachment where purged with dry compressed air to reduce the possibility of atmospheric water or CO_2 contamination of the spectra and samples. The spectra presented are an average of 256 scans. All spectra were recorded at room temperature, approximately 23 ± 0.5 °C, with a resolution of 2 cm^{-1}.

Great care was taken to ensure that the SAMs being characterized were chemisorbed and not physisorbed species. Physisorbed molecules were removed by 30 s of sonication in THF. For glovebox and electroreduction samples, sonication did not result in a lowering of the surface coverage and/or contact angle, suggesting a prevalence of chemisorbed SAMs. For SAMs prepared under atmospheric conditions, however, sonication typically resulted in a significant lowering of the surface coverage and/or contact angle. For example, the contact angle for HDT/Co(ox) was ~120° prior to sonication and decreased to 70−90° after sonication. Presumably, hydrogen-bonded/physisorbed molecules are removed during sonication in THF.

Attempts were made to probe the presence of pinholes in SAM layers on magnetic surfaces by performing cyclic voltammetry in the presence of a solution-phase redox couple. Attempts were also

(22) Moulder, J. F. *Handbook of X-Ray Photoelectron Spectroscopy*; Perkin-Elmer Corporation: Waltham, MA, 1992.

Table 1. Surface Coverages of Fc-$(CH_2)_{11}$-SH Adsorbed on Ni, Co, and Fe Thin Films under Glovebox (GB), Electroreduction (ER)[a], and Atmospheric (Atm) Conditions

		surface coverage, $\times 10^{-10}$ mol/cm^2								
		Ni			Co			Fe		
concn, mM	time, days	GB	ER	Atm	GB	ER	Atm	GB	ER	Atm
1	2	3.7±0.1	2.9±0.4	1.1±0.4	1.8±0.4	1.5±0.2	4.6±1.6	0.6±0.1	1.2±0.2	0.8 ±0.1
	9	2.6±0.5		1.7±1.0	3.4±2.3		17.5±7.8	1.1±0.2		0.5 ±0.3
10	2	4.7±0.5	2.7±0.4	2.7±0.4	5.4±3.0	4.7±0.7	2.9±1.0	2.3±1.5	2.3±0.4	1.1 ±0.5
	9	6.0±1.8		1.6±0.4	1.8±0.4		5.0±3.5	1.8±1.0		0.05±0.01

[a] Electroreductions were performed at the minimum applied potential that allowed for maintenance of >1 mA reductive currents for the entire 10 min duration. Following electroreduction, SAM formation was carried out for a 12−18 h period due to reusage of the three-chambered cell.

Table 2. Surface Coverages of Fc-$(CH_2)_{11}$-NC Adsorbed on Ni, Co, and Fe Thin Films under Glovebox (GB), Electroreduction (ER), and Atmospheric (Atm) Conditions[a,b]

	surface coverage, $\times 10^{-10}$ mol/cm^2								
	Ni			Co			Fe		
concn, mM	GB	ER	Atm	GB	ER	Atm	GB	ER	Atm
1	0.90±0.1	0.54±0.2	2.1±0.3(0.37±0.05)	0.23±0.05	0	0.65±0.5 (0)	0	0.19±0.02	0.12±0.02(0.15±0.03)
10	1.7 ±0.5	1.8 ±0.6	3.5±0.8(1.4 ±0.7)	0.54±0.10	0.21±0.05	0.55±0.09(0)	0.67±0.08	0.34±0.05	0.61±0.10(0.85±0.08)

[a] Data in parenthesis involve a 2 day exposure to the solution of isocyanide. The remainder of the glovebox and atmospheric data involve >5 day exposures. Electroreduction exposures were 12−18 h. [b] Electroreductions were performed at the minimum applied potential that allowed for maintenance of >1 mA reductive currents for the entire 10 min duration.

made to quantify the thickness of the SAM layer by spectroscopic ellipsometry. Please see Supporting Information for details.

Results and Discussion

SAM Formation. Thin metal films were prepared by thermal evaporation of 50−100 nm of Ni, Co, or Fe onto a titanium adhesion layer (25 nm) on SiO_x (1 μm)/Si wafers (i.e., M/Ti/SiO_x/Si films). Three different conditions for SAM formation were explored: (1) transfer of M/Ti/SiO_x/Si substrates into an argon-purged SAM molecule solution immediately following thermal evaporation of the thin film under glovebox conditions, (2) a novel electroreduction process as will be discussed below, or (3) immersion of M/Ti/SiO_x/Si substrates into the SAM molecule solution after exposing the film to atmospheric conditions for at least 30 min. Under glovebox and electroreduction conditions, it is anticipated that minimal oxidation of the metal surface occurs prior to and/or during SAM formation. The major difference between these two conditions is that the e-reduced films begin with native oxides, which are then removed electrochemically, while the glovebox surfaces are not exposed to the atmosphere until after SAM formation. In contrast, surface oxidation is expected to occur prior to and during SAM formation for samples prepared under atmospheric conditions. The major advantage of using electroreduction over glovebox conditions is the ability to make devices under atmospheric conditions and to then remove surface oxide electrochemically to allow the formation of good, low-defect SAMs on the ferromagnetic surface.

Our novel electroreduction process is carried out by utilizing a custom-built, three-chamber cell that is maintained under an argon atmosphere the entire time (Figure 1). In the first chamber, the native oxide is removed by electroreduction in aqueous electrolyte by means of a three-electrode cell. The electrolyte for the electroreduction was chosen to be pH > 7 aqueous solution to allow for the use of thin evaporated films by avoiding extensive etching of Ni, Co, and Fe under acidic conditions.[23] Previous literature reports involving electroreduction of Ni and Fe surfaces have almost exclusively been carried out using acidic conditions with bulk metal samples. Extensive etching with bulk metals is not prohibitive, but is highly problematic with evaporated thin films. The electrolyte for Ni and Fe was 0.1 M NaOH (aq), while that for Co was 0.1 M KH_2PO_4 (aq, pH = 8); Co films became visibly etched during exposure to basic aqueous conditions under both argon and atmospheric conditions. The applied potential during the electroreduction was critical for optimizing SAM surface coverages (*vide infra*). After electroreduction of the working electrode for 10 min, the substrate was immediately transferred to the second chamber for rinsing with deionized water and then transferred to a third chamber containing the ethanolic solution of either thiol or isocyanide molecules. The contents of each chamber were purged with argon for 2 h prior to electroreduction and the cell was kept under argon during the entire duration of SAM formation to prevent reoxidation of the metal surface.

Surface Coverage. The extent of SAM formation was probed by either cyclic voltammetry, using either (11-thiolundecyl)ferrocene (Fc-$(CH_2)_{11}$-SH) or (11-isocyanoundecyl)ferrocene (Fc-$(CH_2)_{11}$-NC). The surface coverage results from cyclic voltammetry for the ferrocene SAMs (Figure S1) for all three conditions are provided in Tables 1 and 2 and depicted graphically in Figure 2. For comparative purposes, surface coverage data is also provided for Fc-$(CH_2)_{11}$-SH and Fc-$(CH_2)_{11}$-NC SAMs formed on freshly evaporated Au/Ti thin films (Table 3). The peak current from cyclic voltammograms showed a linear dependence with scan rate over the range 0.1−1 V/s consistent with a surface-confined Faradiac process and surface-bound redox species.[11] As the data shows, surface coverages for all three metals were generally higher when Fc-$(CH_2)_{11}$-SH was used, especially for Co and Fe, which showed vanishingly low

(23) *CRC Handbook of Chemistry and Physics*, 88th ed.; Lide, D. R., Ed.; CRC Press: Boca Raton, FL, 2007−2008.

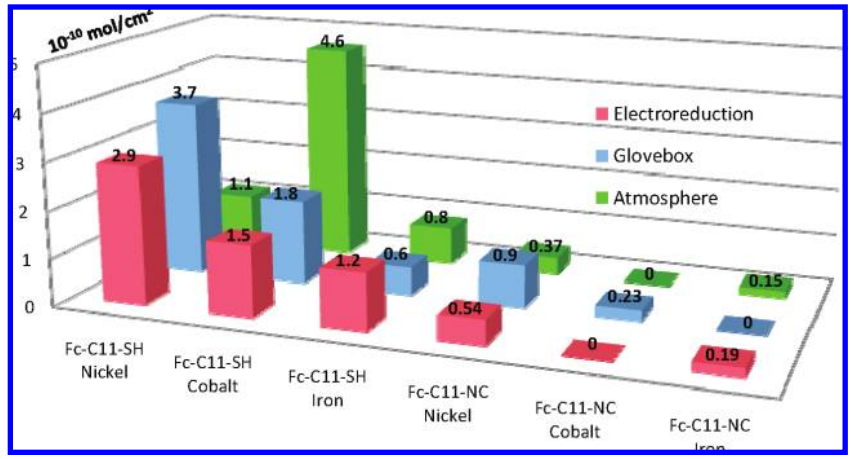

Figure 2. Surface coverage of SAMs on Ni, Co, and Fe surfaces prepared from 1 mM SAM molecule solutions. Glovebox and atmosphere samples were prepared over a 2 day period; electroreduction samples were soaked in the SAM molecule solution for 12−18 h.

Table 3. Surface Coverages and Contact Angles on Gold Thin Films

SAM	concn, mM	surface coverage, $\times 10^{-10}$ mol/cm^2	contact angle, deg
Fc-$(CH_2)_{11}$-SH	1	5.6±0.5	
Fc-$(CH_2)_{11}$-NC	1	1.8±0.4	
C_{16}SH	1		111.0
C_{16}NC	10		77.5

Table 4. Contact Angles for Ni, Co, and Fe Thin Films Soaked in Ethanolic Hexadecanethiol or Hexadecaneisocyanide Solutions under Glovebox (GB), Electroreduction (ER)[a], and Atmospheric (Atm) Conditions[d]

		contact angle, deg								
		Ni			Co			Fe		
SAM	concn, mM	GB	ER	Atm	GB	ER	Atm	GB	ER	Atm
C_{16}SH	1	100.4	68.0	43.9	110.7	63.4	73−83[a]	48.5	53.0	43.7
	10	107.3	92.9	68.8	112.5	79.1	74−94[b,c]	89.2	73.3	76.1[c]
C_{16}NC	1	39.1	48.8	35.6	57.6	25.5	43.9	44.3	64.8	51.0
	10	87.8	66.1	49.7	40.1	52.0	44.4	57.8	64.8	77.7

[a] Electroreductions were performed at −1.2 V vs Ag/AgCl for 10 min. [b] Contact angles were examined over several days and fluctuated with time. [c] Etching of the surface occurs over time. [d] The contact angle data reported are averages of 4−8 contact angles; standard deviations fall within the range ±0.5−2.0.

surface coverages with Fc-$(CH_2)_{11}$-NC. This is consistent with literature findings that isocyanide-functionalized molecules bind appreciably well to Ni surfaces.[11] For Fc-$(CH_2)_{11}$-SH, the surface coverages for electroreduced surfaces are comparable to those prepared in the glovebox. Relative to the "gold standard", the surface coverages for glovebox and electroreduction samples are typically less than a factor of 2 lower. Increasing the Fc-$(CH_2)_{11}$-SH concentration improves the surface coverage for electroreduced Co, electroreduced Fe, and glovebox Ni. Atmospheric conditions for Ni and Fe typically gave surface coverages that were lower than that for electroreduced or glovebox conditions. The exceptions are Ni (1 mM, 9 day) and Fe (10 mM, 2 day), which show higher atmospheric surface coverages than expected. Surprisingly, atmospheric conditions for Co (1 mM, 9 days) gave coverages that were an order of magnitude (1.8×10^{-9} mol/cm^2) higher than that for glovebox or electroreduction conditions. We ascribe this to unexpectedly high etching rates of CoO_x/Co by Fc-$(CH_2)_{11}$-SH, which result in significant roughening of the surface over time as corroborated by AFM measurements.[11,12] Interestingly, Co (atmosphere) treated with 10 mM Fc-$(CH_2)_{11}$-SH over nine days results in more typical surface coverages on the order of 10^{-10} mol/cm^2. For both Co and Fe surfaces prepared under atmospheric conditions over a nine day period in 10 mM solutions, the surfaces become visibly etched and pitted, which may explain the lower-than-expected surface coverages.

Contact Angle. Comparisons between the three methods for SAM formation were also made with HDT and HDI using contact angle measurements (Table 3). High contact angles approaching or equal to that of HDT on Au (111°) were obtained for HDT on Ni and Co at both 1 and 10 mM SAM molecule concentrations under glovebox conditions, suggesting excellent SAM formation and alkyl chain alignment. For Fe, the contact angle for HDT was significantly lower (49°) at 1 mM concentrations but improved markedly for 10 mM concentrations (89°). Under electroreduction conditions, 10 mM HDT concentrations were required to achieve appreciably high contact angles for all three surfaces. The contact angles for HDT on e-reduced films were surprisingly low when considering the high surface coverages observed for Fc-$(CH_2)_{11}$-SH under identical conditions and the low surface oxide content for electroreduced films observed by XPS (*vide infra*). AFM studies (Figure 3) clearly show that the root-mean-square (rms) surface roughness of postelectroreduction Ni and Co films without SAMs increases relative to that for freshly evaporated thin films (Ni, 1.5 to 2.2 nm; Co, 0.89 to 1.2 nm). For Fe, the rms surface roughness decreases slightly after 10 min of electroreduction from 1.7 to 1.6 nm; however, the lower contact angle for HDT on electroreduced films is most likely a result of higher surface oxide content according to XPS (*vide infra*). Hence, we attribute the lower contact angles for electroreduced Ni and Co to increased surface roughness, which disturbs the long-range crystalline order of the SAM and affects the wetting behavior. For all three ferromagnetic surfaces, as well as gold, HDT gave significantly higher contact angles than HDI. This is consistent with inferior crystallinity of HDI SAMs but could also be due to lower SAM densities, as suggested by the ferrocene surface coverage data. It is clear that increasing the HDI solution concentration results in higher contact angles in most cases. HDI on Ni gave higher contact angles than the same on Co and Fe, which further corroborates the

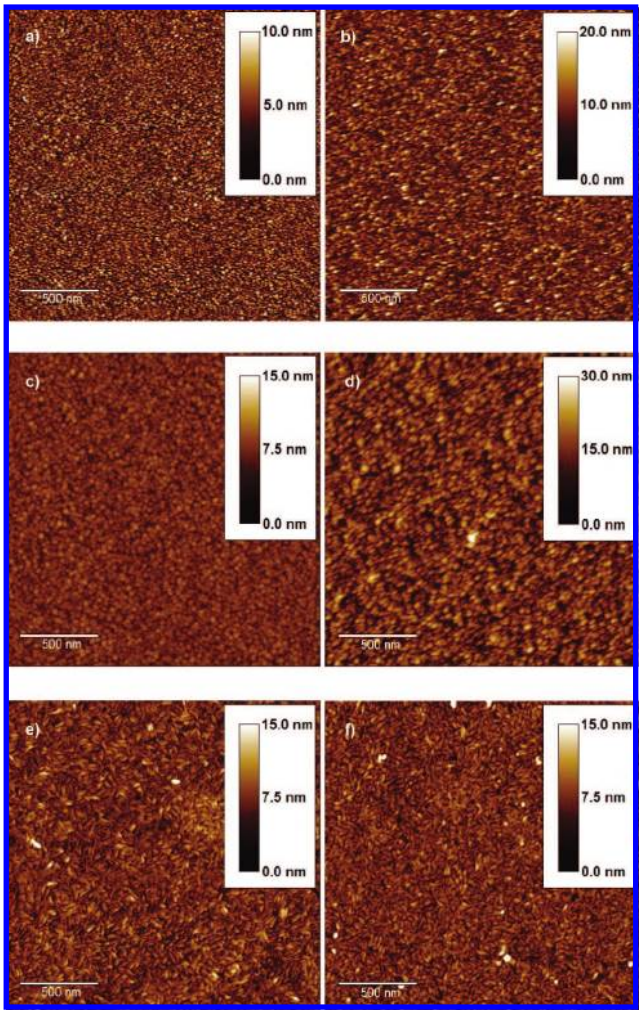

Figure 3. Atomic force microscopy images of bare nickel (a), electroreduced nickel (b), bare cobalt (c), electroreduced cobalt (d), bare iron (e), and electroreduced iron (f). Scale bar: 500 nm.

claim that isocyanides bind preferably to Ni surfaces. For Ni and Fe, HDT SAMs did not apparently form well under atmospheric conditions. Interestingly, the contact angle for HDT on Co under atmospheric conditions showed time-dependent behavior; the contact angle decreases from 94 to 74° over a four day period (Figure S2). This is consistent with etching of the Co surface by HDT over time, which leads to a rougher film. Over time, crystals form on the surface and in solution. Centrifugation followed by dissolution of the crystals in a minimal amount of THF affords a pale purple solution indicative of a Co^{II} complex, presumably $Co(HDT)_x$. This observation will be further explored in future studies and suggests the etching mechanism involves air oxidation of Co surface atoms followed by complexation by HDT.

XPS. X-ray photoelectron spectroscopy (XPS) was used to determine the extent of oxide formation before and after hexadecanethiol SAM formation for glovebox and electroreduction conditions. Samples prepared under atmospheric conditions were studied by XPS to a lesser extent because of inferior surface coverage and contact angle data. Bare Ni, Co, and Fe surfaces were analyzed as references. Bare Ni showed a broad (fwhm = 2.1) O 1s peak at 531.8 eV (% area = 64.4%), a narrower peak (fwhm = 1.0) at 529.6 eV (% area = 30.1%), and a broad peak at 532.8 eV (% area = 5.5%; Figure 4). These peaks are assigned to $Ni^{2+}(OH)_2$, NiO, and surface contaminants (H_2O, C−O containing organics, and CO_2), respectively.[24,25] Bare Co showed similar peaks with the same binding energies and assignments with similar distributions. Bare Fe showed a broad (fwhm = 2.0) O 1s peak at 531.7 eV (% area = 50.1%) along with a narrower peak (fwhm = 1.1) at 530.2 eV (% area = 49.9%) assigned as $Fe^{2+}(OH)_2$ and Fe_3O_4, respectively.[24] The metal $2p_{3/2}$ spectral regions for all three bare ferromagnetic films showed evidence of a highly oxidized surface especially in the case of Fe as indicated by the presence of intense peaks at slightly higher binding energy than the pristine metal $2p_{3/2}$ peaks at 852.7 eV (Ni), 778.3 eV (Co), and 707 eV (Fe; Figure 5).[22] After these samples were Ar ion sputtered for 10 min in situ, the intensities of the O 1s band decreased significantly by a factor of ~7.5 and the metal $2p_{3/2}$ spectral regions were consistent with pristine, nonoxidized metal surfaces. The O 1s and metal $2p_{3/2}$ spectral regions for hexadecanethiol (10 mM) glovebox and electroreduction samples were then compared to that of bare and sputtered metal surfaces. *The intensities of the O 1s bands for Ni and Co glovebox and electroreduction samples were comparable to that of the sputtered bare surfaces indicating that these films have very low surface oxygen content.* The oxygen content of glovebox and electroreduced Fe surfaces was significantly higher and only showed slightly lower oxygen levels than the bare surface with native oxide. Interestingly, the electroreduced Fe sample showed lower amounts of Fe_3O_4 than glovebox and bare surfaces but greater amounts of $Fe^{2+}(OH)_2$. The metal $2p_{3/2}$ spectral regions corroborate the findings from the O 1s data: electroreduced Ni and Co show high intensity pristine metal $2p_{3/2}$ peaks with low intensity peaks at 856.0 and 781.5 eV, respectively; glovebox Ni and Co show signs of shoulders at slightly higher binding energies than the pristine metal $2p_{3/2}$ peaks; and the metal $2p_{3/2}$ spectra for glovebox and electroreduced Fe are practically superimposable with that of bare Fe. Importantly, the XPS data clearly shows that the electroreduction process effectively removes oxide/hydroxide from a surface that has been exposed to atmospheric conditions. This supports our claim that electroreduction can be utilized as a process step during the construction of molecular electronic devices under atmospheric conditions. Low surface oxide/hydroxide content at the SAM/ferromagnetic surface is expected to play a crucial role in charge transport in metal−insulator−metal device architectures.

Time Dependence of Electroreduction. The aforementioned XPS data was attained after 10 min of electroreduction at the minimum potential that could maintain the current at >1 mA for the entire duration. Atomic force microscopy performed on Ni and Co freshly evaporated surfaces and electroreduced surfaces without SAMs showed that electroreduction causes a ~40% increase in surface roughness. This increased roughness is attributed to etching of the surface during the electroreduction process. SAMs that are formed on surfaces with roughnesses on the same order as the length of the molecular monolayer are expected to have larger defect densities and poor crystallinity. Thus, it is important to control surface roughening during the electroreduction process. To this end, we studied electroreduction as a function of time. First, we examined how the surface coverage for Fc-$(CH_2)_{11}$-SH varied with the time of the electroreduction (Figure 6). For Ni, the surface coverage

(24) Bhargava, G.; Gouzman, I.; Chun, C. M.; Ramanarayanan, T. A.; Bernasek, S. L. *Appl. Surf. Sci.* **2007**, *253*, 4322.
(25) Dupin, J.-C.; Gonbeau, D.; Vinatier, P.; Levasseur, A. *Phys. Chem. Chem. Phys.* **2000**, *2*, 1319.

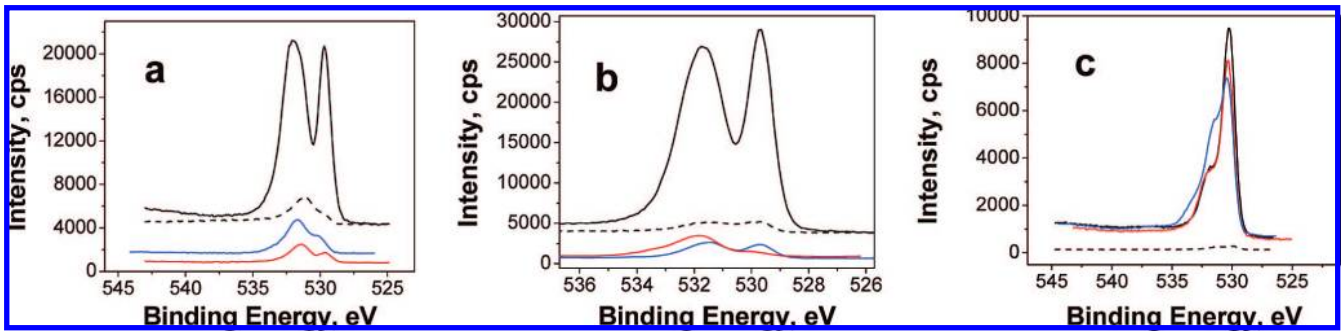

Figure 4. XPS O 1s regional scans for (a) Ni, (b) Co, and (c) Fe bare surfaces (black line), bare surfaces after 10 min in situ Ar ion sputter treatment (black dashed line), 10 mM hexadecanethiol SAMs prepared in the glovebox (red line), and 10 mM hexadecanethiol SAMs prepared after 10 min electroreduction (blue line).

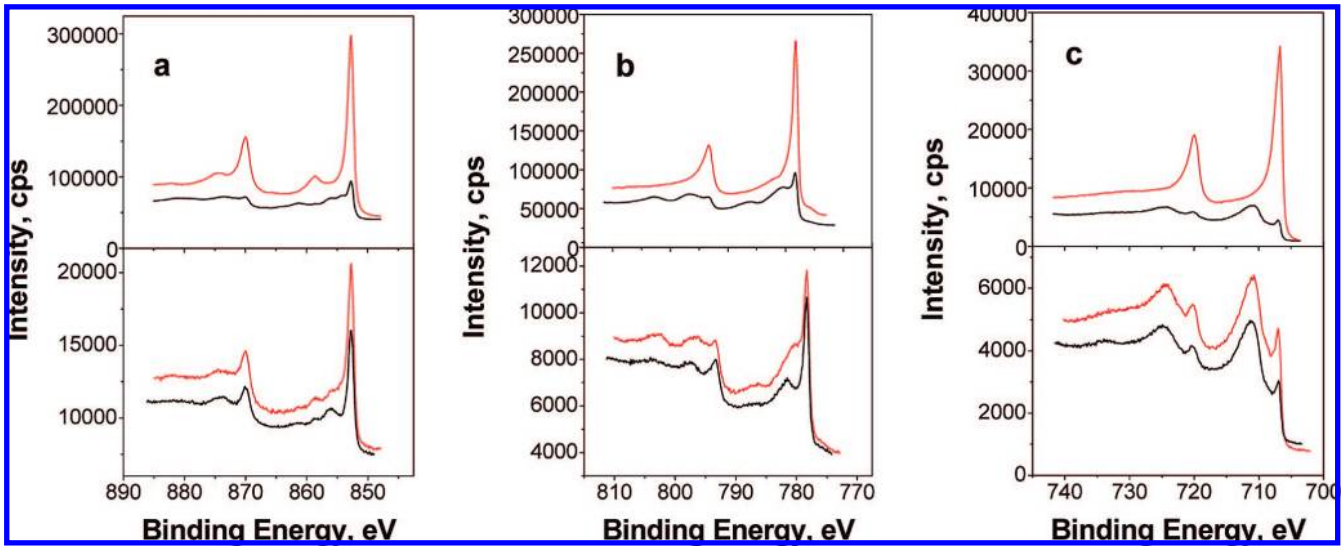

Figure 5. XPS metal 2p regional scans for (a) Ni, (b) Co, and (c) Fe bare surfaces (upper plot, black line), bare surfaces after 10 min in situ Ar ion sputter treatment (upper plot, red line), 10 mM hexadecanethiol SAMs prepared in the glovebox (lower plot, red line), and 10 mM hexadecanethiol SAMs prepared after 10 min electroreduction (lower plot, black line).

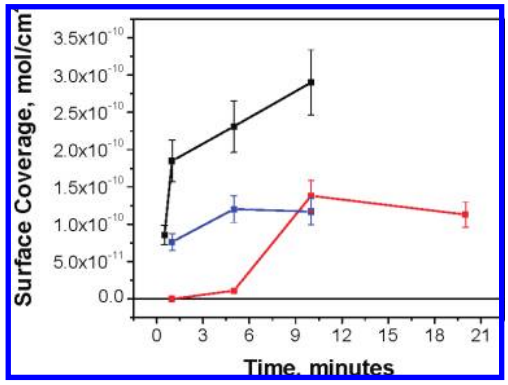

Figure 6. Surface coverages of Fc-$(CH_2)_{11}$-SH as a function of the duration of electroreduction at −1200 mV vs Ag/AgCl reference electrode for nickel (black line with squares), cobalt (red line with squares), and iron (blue line with squares).

increases sharply at $t > 30$ s and then increases less dramatically up to 10 min. For Fe, the surface coverage remains fairly constant as a function of electroreduction time. Surface coverages for Co appear to abide by a sigmoidal function showing a rapid increase in surface coverage between 5 and 10 min. Because the surface roughness from AFM only increases by ~40% for Ni and Co between $t = 0$ and $t = 10$ min and actually decreases slightly for Fe, the surface coverage improvement at longer electroreduction times is most likely a result of more complete surface oxide removal. The surface coverage data is consistent with O 1s and metal $2p_{3/2}$ XPS data performed as a function of electroreduction time (Figures S3, S4). For Ni, maximum oxide/hydroxide removal from the surface occurs after 5 min of electroreduction. For Co, 10 min of electroreduction appears to be necessary to achieve minimal surface oxygen content. For Fe, the lowest oxygen/oxidized Fe levels occurs at 1 min of electroreduction and increases slightly for longer electroreduction times, which is consistent with the low variance of the time-dependent surface coverage data.

Applied Potential Dependence of Electroreduction. The optimal applied potential used during the 10 min electroreduction was also studied for Ni, Co, and Fe by determining the surface coverage of Fc-$(CH_2)_{11}$-SH after submersion of the electroreduced sample in a 1 mM ethanolic solution (Figure 7). A clear plateau in surface coverage is reached beyond −1.0 V versus Ag/AgCl for both Ni and Co. In the case of Fe, the surface coverage reaches a maximum at −1.2 V versus Ag/AgCl and then dramatically plummets. The critical potential appears to coincide with prevalent hydrogen evolution at the working electrode; below this potential, bubble formation does not occur to a large extent. It is known from the literature that

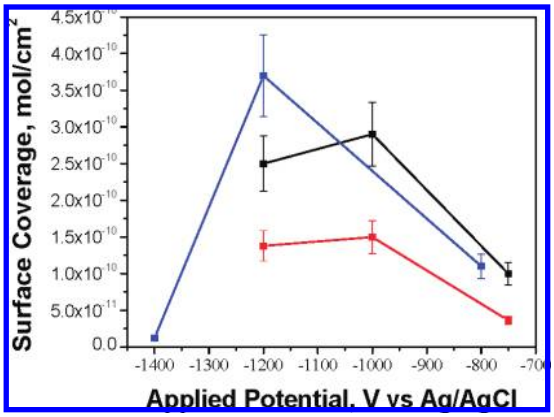

Figure 7. Surface coverages of Fc-$(CH_2)_{11}$-SH as a function of the applied potential during electroreduction for nickel (black line with squares), cobalt (red line with squares), and iron (blue line with squares).

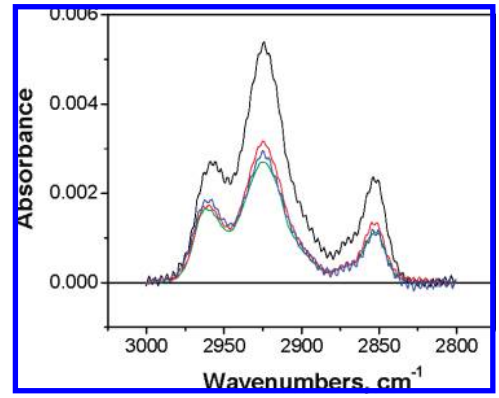

Figure 8. Reflectance-absorbance infrared spectra for hexadecanethiol on electroreduced nickel (black line), cobalt (red line), and iron (blue line) as well as on evaporated gold (green line).

hydrogen atoms are facile surface oxide etchants.[26–30] Thus, we propose that the surface oxide is removed by electroreduction via one or both of the following mechanisms:

$$\mathrm{NiO/Ni} + \mathrm{H_2O} + e^- \rightarrow \mathrm{H(ads)/NiO/Ni} + {}^-\mathrm{OH} \qquad (1)$$

$$\mathrm{2H(ads)/NiO/Ni} \rightarrow \mathrm{H_2O} + \mathrm{Ni^0/Ni}$$

$$\mathrm{Ni(OH)_2/Ni} + \mathrm{2H_2O} + 2e^- \rightarrow \mathrm{2H(ads)/Ni(OH)_2/Ni} + 2\,{}^-\mathrm{OH} \qquad (2)$$

$$\mathrm{2H(ads)/Ni(OH)_2/Ni} \rightarrow \mathrm{2H_2O} + \mathrm{Ni^0/Ni}$$

Beyond −1.2 V, the surface coverage on Fe dramatically plummets to $\sim 1 \times 10^{-11}$ mol/cm^2. The cause of this may be due to the fact that at −1.4 V, O_2 evolution at the Pt counterelectrode becomes increasingly rapid. Thus, the solution O_2 concentration increases, allowing for surface reoxidation either during electroreduction or immediately after the applied potential is removed. Fe oxidation is known to be quite facile. The results are consistent with Fe being more susceptible to reoxidation than both Ni and Co. One way to avoid reoxidation of the electroreduced surface is to purge the solution rapidly with argon during the electroreduction process. When this is performed in the case of −1.4 V for Fe for 10 min, the surface coverage dramatically improves to 1.4×10^{-10} mol/cm^2.

Surface IR. Hexadecanethiol SAM formation on Ni, Co, and Fe under glovebox and electroreduction conditions was studied using reflectance-absorbance infrared spectroscopy (RAIRS). Figure 8 shows the IR spectra for electroreduction samples of hexadecanethiol on Ni, Co, and Fe overlaid with hexadecanethiol on evaporated Au. For HDT on Ni, Co, Fe, and Au, three peaks were observed at 2961, 2925, and 2853 cm^{-1} assigned as the $\upsilon_{as}(CH_3)$, $\upsilon_{as}(CH_2)$, and $\upsilon_s(CH_2)$ stretching modes, respectively.[31] For atmospheric and glovebox conditions, nearly identical spectra with similar absorbances were attained for surface-bound hexadecanethiol (Figure S5). For electroreduction samples, however, the absorbances were sample dependent (Figure S6). For Ni, the absorbance is greatest after 10 min, consistent with XPS and Fc-$(CH_2)_{11}$-SH surface coverage data. For Fe, the highest absorbance was observed with the 1 min electroreduction sample, which is consistent with XPS data which shows lower surface hydroxide/oxide content for the 1 min sample. For Co, the absorbance decreased considerably as the electroreduction time was increased from 1 to 5 to 10 min (Figure S6). This observation may be due to extensive etching of Co during electroreduction which results in thinner films and signal attenuation.

Etching of the Surface. Several observations suggest that etching of the surface occurs in the cases and Co and Fe under atmospheric conditions but is undetectable in the case of Ni. First, crystals form over time on the surface and in solution when Co and Fe surfaces are submerged in 10 mM solutions of HDT or Fc-$(CH_2)_{11}$-SH under atmospheric conditions. Second, the entire ferromagnetic surface becomes visibly etched over long periods of time (>2 weeks) under these conditions leaving behind only the titanium adhesion layer. The etching rates appear to be faster for HDT than Fc-$(CH_2)_{11}$-SH perhaps due to lower solubility of the metal-HDT adducts. Third, the Fc-$(CH_2)_{11}$-SH surface coverage data abides by predictable trends in the case of Ni but not for Co and Fe, which suggests that etching/surface roughening is playing a role in the latter cases. It is interesting to note that Nuzzo and co-workers observed discoloration and pitting when forming short-chain SAMs ($n \leq 3$) on Cu and Ag surfaces and that prolonged exposure resulted in dissolution of the metal.[32]

SAM Stability. The stability of SAMs on ferromagnetic surfaces upon extended exposure to atmospheric conditions is an important consideration for implementation of these molecular monolayers into real devices. XPS was used to examine the stability of hexadecanethiol (10 mM) SAMs prepared under glovebox and electroreduction conditions over the course of several days to weeks. For glovebox and electroreduction samples exposed to atmospheric conditions on the 1−2 h time scale, the XPS data shows a S 2p peak at ~162 eV consistent with a metal-bound thiolate species (Figure 9, S7).[32] Over time, the sulfur atom becomes increasingly oxidized to a S═O containing species (e.g., sulfonate, sulfinate, sulfone), as shown by the appearance of a S 2p peak at ~169 eV.[32] After five days,

(26) Hase, A.; Gibis, R.; Kunzel, H.; Griebenow, U. *Appl. Phys. Lett.* **1994**, *65*, 1406.
(27) Eyink, K. G.; Grazulis, L. *J. Vac. Sci. Technol., B* **2005**, *23*, 554.
(28) Akatsu, T.; Plossl, A.; Stenzel, H.; Gosele, U. *Proc. - Electrochem. Soc.* **2001**, *99*, 60.
(29) Kagadei, V. A.; Proskurovskii, D. I.; Romas, L. M. *Russ. Microelectron.* **1998**, *27*, 91.
(30) Ohashi, T.; Saito, Y.; Maruyama, T.; Nanishi, Y. *J. Cryst. Growth* **2002**, *237−239*, 1022.
(31) Nuzzo, R. G.; Dubois, L. H.; Allara, D. L. *J. Am. Chem. Soc.* **1990**, *112*, 558.
(32) Laibinis, P. E.; Whitesides, G. M.; Allara, D. L.; Tao, Y.-T.; Parikh, A. N.; Nuzzo, R. G. *J. Am. Chem. Soc.* **1991**, *113*, 7152.

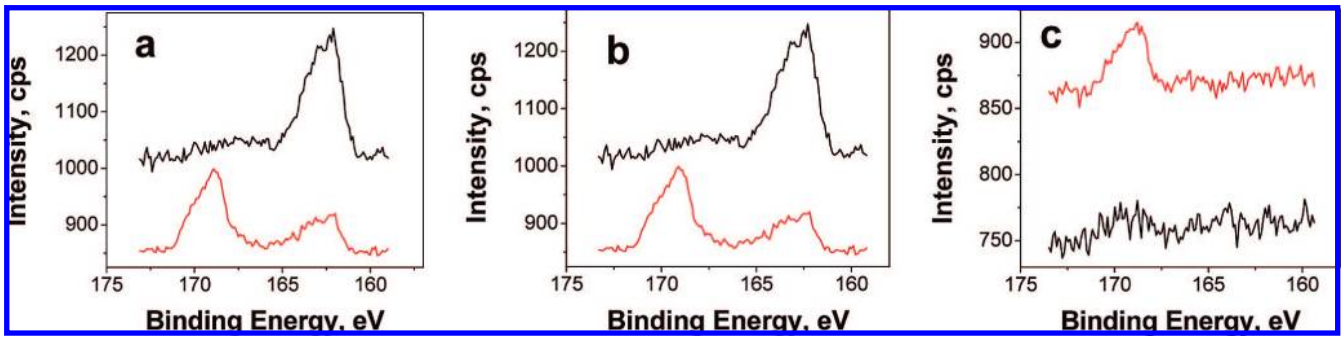

Figure 9. XPS S 2p regional scans for hexadecanethiol on electroreduced (a) Ni, (b) Co, and (c) Fe after minimal exposure to atmospheric conditions (black line) and after 5 days constant exposure to atmospheric conditions (red line).

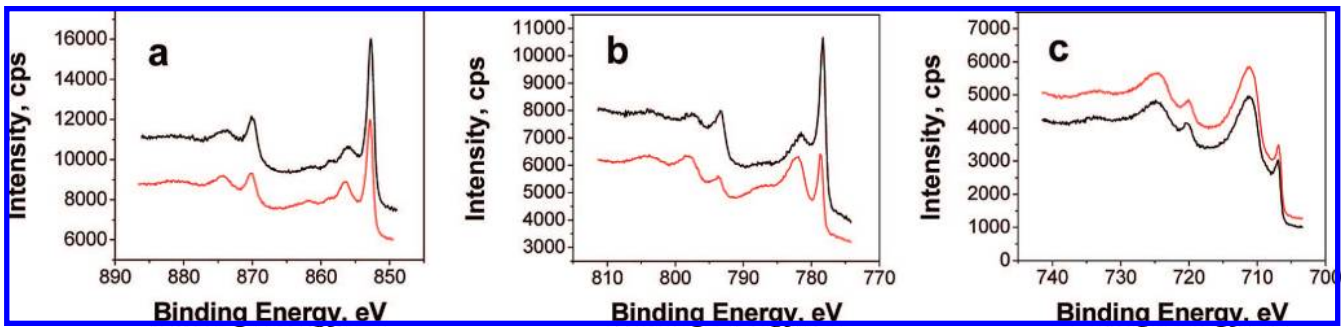

Figure 10. XPS metal 2p regional scans for hexadecanethiol on electroreduced (a) Ni, (b) Co, and (c) Fe after minimal exposure to atmospheric conditions (black line) and after five days constant exposure to atmospheric conditions (red line).

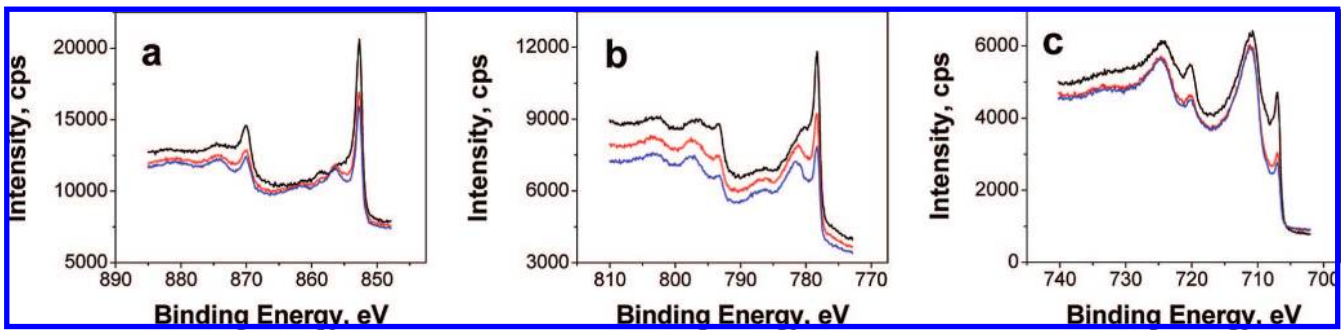

Figure 11. XPS metal 2p regional scans for hexadecanethiol SAMs on (a) Ni, (b) Co, and (c) Fe prepared in the glovebox after minimal exposure to atmospheric conditions (black line), after 8 days constant exposure to atmospheric conditions (red line), and after 15 days constant exposure to atmospheric conditions (blue line).

the Ni and Co electroreduced samples contain both oxidized and nonoxidized sulfur with the latter predominating. After eight days, glovebox Ni and Fe samples contain a mixture of oxidized and nonoxidized sulfur atoms, while the Co sample's sulfur atoms have become almost entirely oxidized.

By focusing on the metal 2p spectral regions, the kinetics of oxidation of the surface metal atoms in the presence of a SAM overlayer can be attained (Figures 10 and 11). Electroreduced Co appears to reoxidize more rapidly than electroreduced Ni over a five day period as observed by the attenuation of the pristine Co peak at 778.3 eV and growth of an equally intense broad peak at 782 eV (attributed to oxidized Co, or Co(ox); Figure 10). For Ni, surface oxidation appears to occur more slowly as is evident from only a slight increase in the intensity of the Ni(ox) peak at 856.3 eV. In fact, the intensity ratio for the pristine Ni peak at 852.7 eV to the Ni(ox) peak at 856.3 eV only decreases from 1.5 to 1.3 over a five day period. For electroreduced Fe, the 1 h and 5 day spectra are nearly superimposable, indicating only a minor change in the oxidation of the Fe surface atoms. Oxidation of Ni and Co surfaces appears to occur more slowly for samples prepared in the glovebox than those prepared by electroreduction by comparing the relative intensities of the pristine and M(ox) peaks over time (Figure 11). For glovebox Co, the intensity ratio decreases to 1.2 over 8 days, while that for Ni decreases to 1.4. For glovebox Fe, the surface at $t = 1$ h is noticeably less oxidized than the related electroreduced sample (intensity ratio 0.75 vs 0.61, respectively). As a result, the surface of the glovebox Fe sample showed signs of oxidation over time.

Additional insights into the oxidation of the surfaces over time were attained by analyzing the XPS O 1s spectral region and fitting the curves to the sum of three Lorentzian−Gaussian functions centralized at ~533, ~531.5, and 529.5 eV (Ni and Co, 530.1 eV for Fe; Figures S8, S9, Table S1). The peaks at ~530 eV were attributed to O^{2-}-containing species, NiO, CoO, or Fe_3O_4, while the broader peak at 533 eV was attributed to the adsorption of H_2O, C−O containing organics, and/or CO_2 to the surface.[24,25] The intensities of both of these peaks remain

fairly constant over extended periods on time in the ambient. The ~531.5 eV species were assigned to the presence of $M^{2+}(OH)_2$ species as previously mentioned. Both glovebox Ni and Co exhibit a marked increase (~factor of 3) in the intensity of the ~531.5 eV peak over time. Meanwhile, electroreduced Ni and Fe show negligible changes in intensity of the ~531.5 eV peak, while glovebox Fe and electroreduced Co show noticeable but relatively minute intensity increases at this binding energy over time. Because the O 1s peak intensities at ~531.5 eV increase over time while those at ~530 eV remain constant for Ni and Co, we attribute the increases in intensity of the metal $2p_{3/2}$ spectral region at ~856.0 and ~781.5 eV, respectively, to oxidation of surface atoms to $M^{2+}(OH)_2$ species for both glovebox and electroreduction cases.

Conclusion

In conclusion, we have examined SAM formation of thiols and isocyanides on Ni, Co, and Fe thin films under inert and atmospheric conditions. We found that isocyanides form decent SAMs on Ni while thiols form good layers on all three surfaces, especially for Ni and Co. We developed a novel, broadly applicable electrochemical technique to remove native oxides of ferromagnetic surfaces, facilitating the formation of high surface coverage SAMs on thin, evaporated metal films that have been pre-exposed to atmospheric conditions. The SAMs prepared under electroreduction conditions rival those prepared under inert conditions in a glovebox prior to exposure to the ambient. Overall, this study comprises an important step toward the development of molecular electronic devices that utilize self-assembled monolayers on ferromagnetic surfaces with low surface-oxide content.

Acknowledgment. This work was supported by the University of North Carolina at Chapel Hill and the NSF (ECCS-0707315). We would also like to thank Carrie Donley for help with countless hours of XPS, Simon E. Lappi for help with conducting RAIRS experiments, Peter S. White for running XRD samples, and John Tumbleston of the UNC Physics Department for help with ellipsometry.

Supporting Information Available: Detailed synthesis of all molecules. This material is available free of charge via the Internet at http://pubs.acs.org.

JA800278A